InAs/$Ga_{1-x}In_xSb$ strained-layer superlattices grown by molecular-beam epitaxy

D. H. Chow
T. J. Watson Sr. Laboratory of Applied Physics, California Institute of Technology, Pasadena, California 91125

R. H. Miles
Hughes Research Laboratories, Malibu, California 90265

J. R. Söderström[a] and T. C. McGill
T. J. Watson Sr. Laboratory of Applied Physics, California Institute of Technology, Pasadena, California 91125

(Received 31 January 1990; accepted 21 March 1990)

We report the successful growth of InAs/$Ga_{1-x}In_xSb$ strained-layer superlattices by molecular-beam epitaxy. The superlattices are grown on thick, strain-relaxed InAs or GaSb buffer layers on (100)-oriented GaAs substrates. A short-period, heavily strained superlattice at the GaAs interface is found to improve the structural quality of the buffer layer. Arsenic incorporation in nominally pure GaSb layers is found to depend strongly on substrate temperature and As-background pressure. Best strained-layer superlattice structural quality is achieved for samples grown at fairly low substrate temperatures ($<400\,^{\circ}C$). Photoluminescence measurements indicate that the energy gaps of the strained-layer superlattices are smaller than those of InAs/GaSb superlattices with the same layer thicknesses, in agreement with the theoretical predictions of Smith and Mailhiot [J. Appl. Phys. **62**, 2545 (1987)]. Far-infrared photoluminescence is observed from a 37/25 Å, InAs/$Ga_{0.75}In_{0.25}Sb$ superlattice, demonstrating that far-infrared cutoff wavelengths are compatible with short superlattice periods in this material system.

I. INTRODUCTION

The concept of superlattice infrared detectors was first suggested over ten years ago for the case of HgTe/CdTe superlattices as alternatives to $Hg_{1-x}Cd_xTe$ alloys.[1,2] The advantages of superlattices over bulk materials derive mainly from the fact that layer thicknesses determine superlattice energy gaps, while compositional control is used to select energy gaps in bulk alloys. Epitaxial growth techniques, such as molecular-beam epitaxy (MBE), have made precise layer thickness control possible (to one monolayer in many cases). Hence, superlattices offer improved cutoff wavelength control and uniformity. Furthermore, effective masses can be selected to reduce leakage currents in a superlattice without altering its energy gap. In addition to HgTe/CdTe superlattices, InSb/$InAs_xSb_{1-x}$ strained-layer superlattices have been proposed[3] and studied[4,5] as candidates for infrared detection applications. These (type II) superlattices would allow the extension of III–V growth and processing technology to wavelength ranges unavailable in bulk III–V materials. However, all experimental reports to date of far-infrared cutoff wavelengths in InSb/$InAs_xSb_{1-x}$ superlattices have involved relatively thick layers ($\geqslant$75 Å).[4,5] These thick layers degrade optical absorption significantly, as they increase the spatial separation between electrons and holes in the superlattice.

Recently, it has been proposed that InAs/$Ga_{1-x}In_xSb$ strained-layer superlattices have favorable properties for far-infrared (8–14 μm) detection.[6,7] This material system has type II (staggered) band alignments similar to the heavily studied InAs/GaSb system,[8–14] which is nearly lattice matched. In both cases, the InAs conduction band edge is presumed to be lower in energy than the $Ga_{1-x}In_xSb$ (or GaSb) valence band edge, with a positive superlattice energy gap resulting from quantum confinement of the electrons and holes (when the layers are sufficiently thin). The presence of coherent strain between the InAs and $Ga_{1-x}In_xSb$ layers shifts the band edges such that the superlattice energy gap is reduced. This shift is advantageous because far-infrared cutoff wavelengths can be obtained with reduced layer thicknesses (<35 Å), leading to enhanced absorption and transport properties.[6,7] Thus, the InAs/$Ga_{1-x}In_xSb$ superlattice is a promising III–V alternative for far-infrared detection.

In this paper, we report the successful growth of far-infrared InAs/$Ga_{1-x}In_xSb$ strained-layer superlattices. The samples have been grown by MBE on (100)-oriented GaAs substrates. Structural characterization of the superlattices has been performed by reflection high-energy electron diffraction (RHEED), x-ray diffraction, and transmission electron microscopy (TEM). Far-infrared photoluminescence has been observed, yielding direct measurements of the superlattice energy gaps. Recent measurements of photoconductive response from the samples yield cutoff wavelengths in good agreement with the energy gaps determined by photoluminescence. In addition to exploring potential device applications for InAs/$Ga_{1-x}In_xSb$ superlattices, we have studied more fundamental materials issues which may be of consequence for other semiconductor heterostructures. Techniques for depositing high quality InAs and GaSb buffer layers on GaAs substrates have been explored, in an at-

 0734-211X/90/040710-05$01.00

tempt to provide a nearly lattice matched template for growth of the superlattice. We have also studied the degree to which background As is incorporated into GaSb films at different substrate temperatures, Sb fluxes, and As background pressures.

II. GROWTH

All of our samples have been grown by molecular-beam epitaxy (MBE) on (100)-oriented GaAs substrates in a Perkin Elmer 430 system equipped with both arsenic and antimony crackers. Measurements of the substrate temperature were obtained through a thermocouple in contact with a molybdenum block, to which the substrate was bonded with indium. The thermocouple readings were calibrated to optical pyrometer readings above 500 °C, the As-stabilized to In-stabilized transition during InAs growth, and to the GaAs oxide desorption point. Nominal growth rates were calibrated via bulk film thickness measurements and RHEED oscillations measured during homoepitaxial growth of GaAs and InAs. Bulk GaSb (InSb) growth rates were computed by multiplying the GaAs (InAs) rate by the ratio of the lattice constants of the two materials. A "nude" ion gauge was used to monitor the Sb_2 and As_2 fluxes. Estimates of the absolute As_2 flux were made through residual gas analyzer peak heights calibrated to transitions between the As-stabilized and Ga-stabilized RHEED patterns during growth of GaAs.

III. STRUCTURAL CHARACTERIZATION

A. Buffer layers

Techniques for depositing strain–relaxed InAs and GaSb buffer layers on (100)-oriented GaAs substrates have been explored in an attempt to provide a nearly lattice matched template for growth of the superlattice. For each of the two materials, methods employing severely lattice-mismatched superlattices at the GaAs interface have been tested. Similar schemes have been reported to improve epitaxial layer quality (as determined by surface morphology and electron mobility) in some studies.[15,16] Figure 1 illustrates the layer sequences used for the two types of buffers. For InAs layers, growth commenced with 3000 Å of GaAs at a substrate temperature of 600 °C, followed by a five period, 2 monolayer/2 monolayer, $In_{0.7}Ga_{0.3}As$/GaAs "superlattice" at 520 °C, and a 5000-Å thick InAs layer grown at 450–520 °C. GaSb buffer layers consisted of 3000 Å of GaAs grown at 600 °C, followed by a ten period, 1 monolayer/1 monolayer, GaSb-/GaAs superlattice at 520 °C, and a 5000-Å thick GaSb layer grown at 430–520 °C. Several InAs/$Ga_{1-x}In_xSb$ superlattices have been grown on each of the two types of buffer layers. However, we have generally employed GaSb buffer layers for more heavily strained superlattices ($x \approx 0.25$) because of the intermediate value of the GaSb lattice constant with respect to the two constituent materials.

RHEED patterns observed during growth of the buffer layers became spotty immediately after commencement of the heavily strained superlattices, and regained a streaky appearance after 2 mins (about 300 Å) of growth of the InAs or GaSb bulk layers. The As-stabilized, 2×4 surface reconstruction was observed throughout the InAs layers, while GaSb layers exhibited a characteristic 1×3 RHEED pattern. Cross-sectional TEM has been used to examine threading dislocations in the buffer layers and superlattices. The TEM images reveal dense dislocation networks localized at the GaAs/buffer layer interfaces, with the vast majority of dislocations vanishing within 1000 Å of buffer layer growth. The remaining threading dislocations persist through the buffer layer and superlattice with an approximate density of 10^9 cm^{-2}. In spite of these relatively high dislocation densities, the TEM images reveal smooth, planar InAs/$Ga_{1-x}In_xSb$ superlattice layers over most of the sample area.

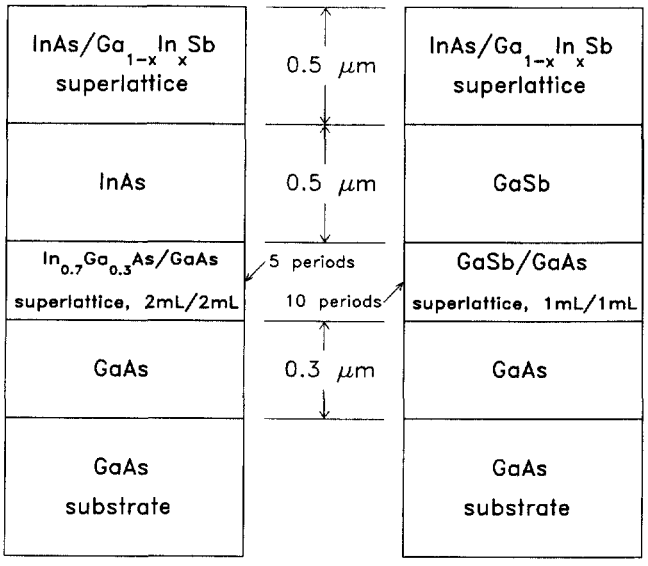

FIG. 1. Schematic layer diagram, illustrating the two buffer layering schemes used to grow InAs/$Ga_{1-x}In_xSb$ superlattices on (100)-oriented GaAs substrates. The left (right) diagram depicts the method used to grow InAs (GaSb) buffer layers.

B. Incorporation of background As in GaSb

X-ray diffraction from InAs/GaSb superlattices grown early in our study suggested that significant quantities of As were incorporated into GaSb layers (i.e., $GaSb_{1-y}As_y$ layers resulted even with the As-shutter closed). Conversely, Sb was not detectable in InAs layers, due largely to the high sticking coefficient of Sb to the closed shutter. In an attempt to minimize the incorporation of As in nominally pure antimonide layers, we grew a series of 2500 Å GaSb films on InAs buffer layers (which were deposited on GaAs substrates by the technique described in the previous section). X-ray diffraction was then used to measure the lattice constant of the resulting layer, resulting in a determination of y. The effects of substrate temperature, background As pressure (varied by changing the As evaporator temperature with the As-shutter closed), and Sb flux were studied.

Figures 2(a) and 2(b) display $\Theta/2\Theta$ x-ray diffraction data from the (400) planes of two $GaSb_{1-y}As_y$ layers grown under different conditions. These two layers represent the maximum and minimum degree of As incorporation

observed in our study (excluding samples grown with the As evaporator turned off). Diffraction peaks from the GaAs substrate and InAs buffer layer are also evident in each figure. The $GaSb_{1-y}As_y$ layer which provided the data shown in Fig. 2(a) was grown at a substrate temperature of 520 °C. A high As-background pressure was created by closing the As shutter, and setting the As evaporator to the temperature needed to maintain an As-stabilized InAs surface at a growth rate of 1 monolayer/s (roughly $As_2/In \approx 10$). As-peak heights (As^+) on the residual gas analyzer in the MBE chamber are approximately five times higher with the As shutter open than with it closed. The data shown in Fig. 2(b)

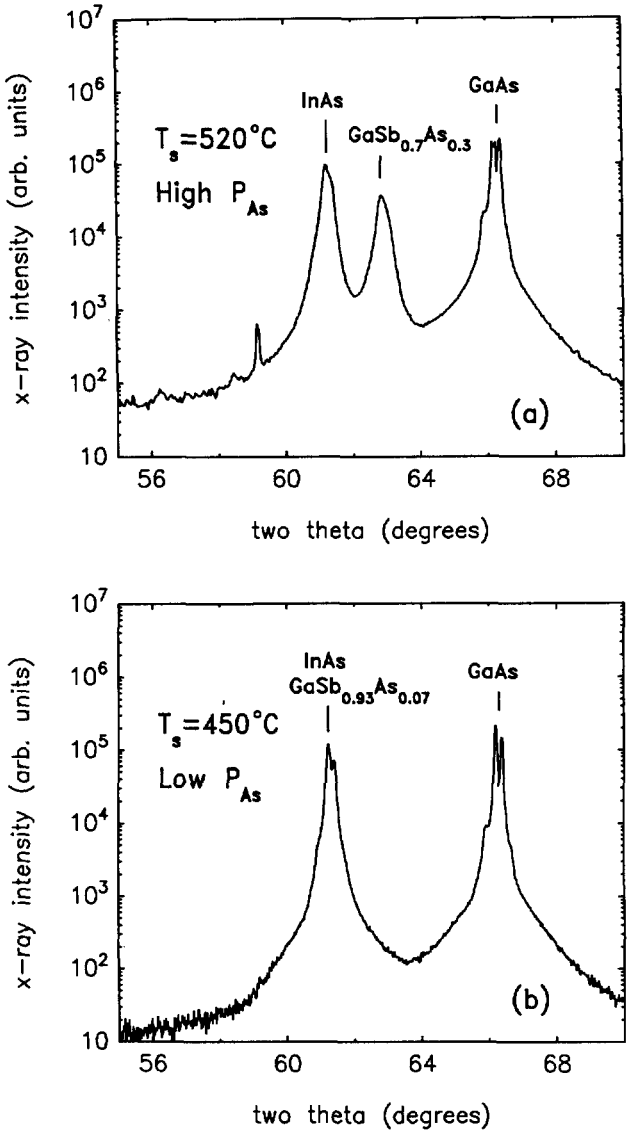

FIG. 2(a) and (b). Θ/2Θ x-ray diffraction data from the (400) planes of two nominally pure (As-shutter closed), 2500-Å thick, GaSb films grown on InAs buffer layers. The samples were irradiated with Cu $K\alpha$ x-rays. In both figures, the InAs buffer layer and GaAs substrate diffraction peaks are labeled. The data displayed in (a) were taken from a sample grown at 520 °C under high As-background conditions. Figure (b) shows data taken from a sample grown at 450 °C under low As-background conditions. The measured lattice constants indicate As mole fractions of 0.3 and 0.07 in (a) and (b), respectively.

were obtained from a $GaSb_{1-y}As_y$ layer grown at 450 °C. The As-background pressure was lowered by reducing the As-evaporator temperature to that needed to maintain an As-stabilized InAs surface at a growth rate of 0.2 monolayer/s. For both samples, a $GaSb_{1-y}As_y$ growth rate of 0.5 monolayer/s was used. The Sb_2 flux was estimated to be a factor of 4 greater than the Ga flux. In fact, our experiments revealed that the magnitude of the Sb_2 flux has no effect on As incorporation as long as it is sufficient to maintain an Sb-stabilized surface. The $GaSb_{1-y}As_y$ diffraction peak shown in Fig. 2(a) is in between the InAs and GaAs peaks, indicating a 30% incorporation of As in the film ($y \approx 0.3$). In contrast, Fig. 2(b) shows a $GaSb_{1-y}As_y$ diffraction peak at approximately the same angle as the peak from the InAs buffer layer, indicating that $y \approx 0.07$. It should be noted that samples grown at substrate temperatures and/or As-background pressures intermediate to those of the two samples discussed here yielded intermediate values of y, with monotonic behavior. These results suggest that As atoms compete strongly with Sb atoms for lattice sites in $GaSb_{1-y}As_y$, and that increasing substrate temperature favors increased As incorporation. Considerably different results have been reported for similar experiments on $InSb_{1-y}As_y$ films.[17,18] It is possible that the cracked arsenic and antimony sources used here yield significantly different sticking coefficients for the two materials than those obtained from tetrameric sources. However, the degree to which As_2 escapes past the closed shutter (during GaSb growth) has not been studied here.

C. Substrate temperature

Several different substrate temperatures have been used for deposition of the InAs/$Ga_{1-x}In_xSb$ superlattice layers, spanning the range 370–450 °C. The superlattices exhibited shiny, smooth surfaces for substrate temperatures < 400 °C, while higher substrate temperatures resulted in hazy, rough surfaces. X-ray diffraction peaks were sharpest and most intense for superlattices grown at 390 °C. It should be noted that we have successfully grown InAs and $Ga_{1-x}In_xSb$ bulk films with good surface morphology at temperatures as high as 525 and 450 °C, respectively. The need for lower growth temperatures in the case of the superlattice may be a result of interdiffusion and/or strain. RHEED patterns observed during growth of the superlattice indicated a 1×3 surface reconstruction for $Ga_{1-x}In_xSb$, and an unusual 2×1 reconstruction for InAs.

Figures 3(a) and 3(b) display Θ/2Θ x-ray diffraction data for two 100 period InAs/$Ga_{0.75}In_{0.25}Sb$ superlattices grown at 390 and 450 °C, respectively. Both structures were grown on GaSb buffer layers, deposited by the method described previously. The intensities of the superlattice satellite peaks shown in Fig. 3(a) are in excellent agreement with those predicted by kinematical theory. The widths of the peaks are limited by the resolution of the x-ray diffractometer used here. The intensity and narrowness of the satellite peaks is indicative of highly regular superlattice growth with limited interdiffusion between layers.[19] In contrast, Fig. 3(b) displays broad peaks (note that the $K\alpha$ doublet is not resolved), and lower superlattice satellite intensities.

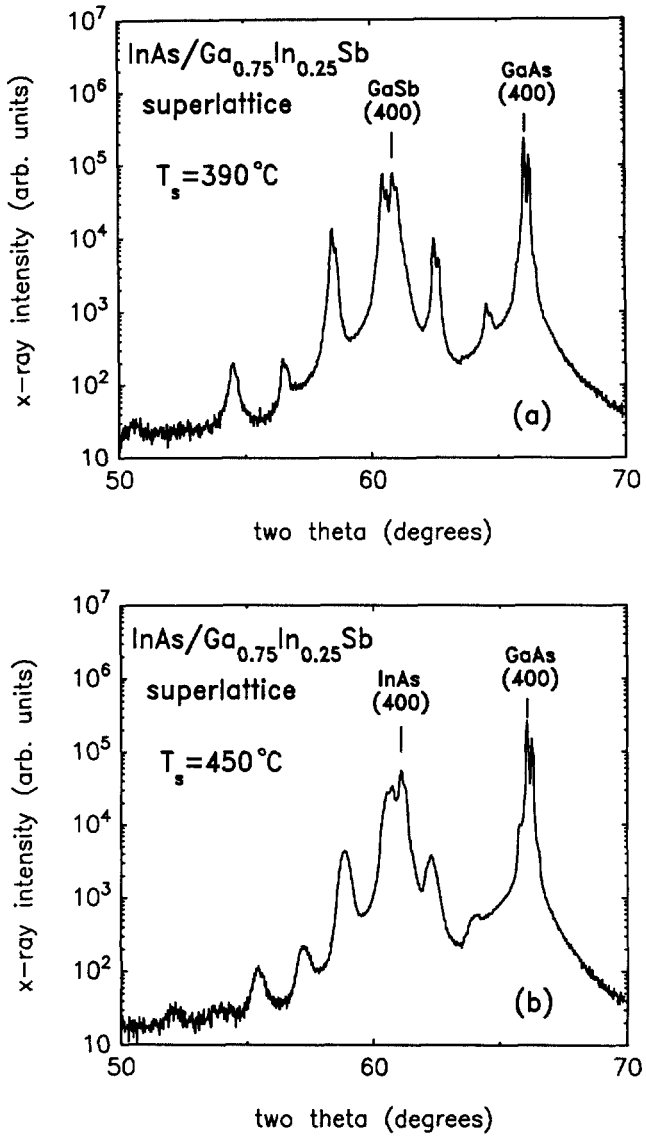

FIG. 3(a) and 3(b). $\Theta/2\Theta$ x-ray diffraction data for two 100 period $InAs/Ga_{0.75}In_{0.25}Sb$ superlattices grown at 390 and 450 °C, respectively, showing (400)-like diffraction peaks. The samples were irradiated with Cu $K\alpha$ x rays. Each peak in figure (a) appears to be bimodal due to the $K\alpha$ doublet, while the peaks in figure (b) are too broad to resolve the doublet. The substrate (GaAs) and buffer layer (GaSb or InAs) peaks are labeled.

IV. OPTICAL CHARACTERIZATION

Photoluminescence spectra from the strained-layer superlattices have been obtained through a Bomem Fourier transform infrared spectrometer (FTIR). Optical excitation was provided by a cooled AlGaAs laser diode or by an Ar ion laser gated by an acousto-optic modulator. The pump sources were chopped at 40 kHz and the detected signal demodulated with a lock-in amplifier prior to passing through the Fourier transform electronics, enabling weak photoluminescence to be separated from background (blackbody) radiation. Luminescence was detected with an InSb detector cooled to 77 K or with a Si:As detector at 4.2 K.

Figure 4 displays photoluminescence spectra from three

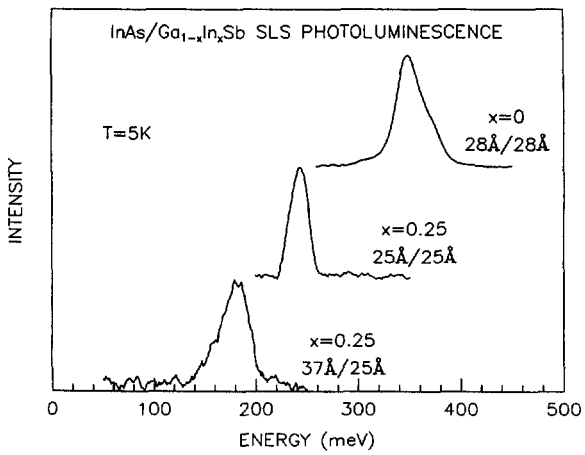

FIG. 4. Photoluminescence spectra from a three $InAs/Ga_{1-x}In_xSb$ superlattices (SL). The top spectrum is from a 28/28 Å SL with $x = 0$, grown on an InAs buffer layer; the middle spectrum is from a 25/25 Å SL with $x = 0.25$, grown on a GaSb buffer layer; and the bottom spectrum is from a 37/25 Å SL with $x = 0.25$, grown on a GaSb buffer layer. All data were taken at 5 K.

$InAs/Ga_{1-x}In_xSb$ superlattices with different layer thicknesses and values of x. Comparison of the top two spectra in the figure demonstrates that the energy gap of an $InAs/Ga_{0.75}In_{0.25}Sb$ superlattice is significantly lower than that of an InAs/GaSb superlattice with slightly greater layer thicknesses. It should be noted that the measured luminescence in the top spectrum is in excellent agreement with previously reported optical measurements from InAs/GaSb superlattices with similar layer thicknesses.[8,9] Furthermore, all of the photoluminescence spectra are in good agreement with the energy gap calculations of Mailhiot and Smith.[6,7] The shift of the strained-layer superlattice energy gap to longer wavelengths is important because good infrared detection requires thin superlattice layers for strong optical absorption (in a type II superlattice) and good transport properties. It is likely that the shift is due to strain-induced movement of the band edges and/or a favorable valence band offset between InSb and GaSb. In either case, increasing the value of x should further reduce the $InAs/Ga_{1-x}In_xSb$ superlattice cutoff wavelength. The bottom photoluminescence spectrum in Fig. 4 displays a low energy edge at 140 meV, or approximately 9 μm. This result demonstrates that cutoff wavelengths in or approaching the far-infrared range are obtainable for $InAs/Ga_{1-x}In_xSb$ superlattices with thin layers (< 40 Å). Furthermore, we have recently measured the photocurrent generated in the superlattices under an external bias as a function of incident photon energy. The spectra are characterized by sharp photocurrent turn ons at threshold energies which are in good agreement with the photoluminescence spectra in Fig. 4. Additional samples which do not give measureable luminescence have shown photoconductive response as far out as 15 μm.

V. CONCLUSIONS

In conclusion, we have successfully grown $InAs/Ga_{1-x}In_xSb$ strained-layer superlattices on GaAs sub-

strates. Techniques for depositing strain-relaxed InAs and GaSb buffer layers have been explored in an attempt to provide nearly lattice matched templates for growth of the superlattices. Good results have been obtained with a method which employs a short period, heavily strained superlattice at the GaAs/buffer layer interface. Incorporation of As in nominally pure GaSb layers has been found to depend strongly on substrate temperature and As-background pressure. Excellent surface morphology and x-ray diffraction data were obtained for strained-layer superlattices grown on GaSb buffer layers at relatively low substrate temperatures (<400 °C). Samples grown at higher substrate temperatures exhibited rough surfaces and weak x-ray diffraction. Photoluminescence spectra from strained-layer InAs/$Ga_{0.75}In_{0.25}Sb$ superlattices reveal energy gaps which are significantly lower than those of InAs/GaSb superlattices with similar layer thicknesses, in good agreement with the theoretical predictions of Mailhiot and Smith.[6,7] Furthermore, we have observed far-infrared luminescence from InAs/$Ga_{1-x}In_xSb$ superlattices with short periods (<65 Å). Recent photoconductivity spectra show photocurrent threshold energies (cutoff wavelengths) out to 15 μm from superlattices with periods less than 75 Å. These results suggest that large optical absorption coefficients, which are theoretically obtainable only for thin layers in a type II superlattice, are compatible with far-infrared cutoff wavelengths in this material system.

ACKNOWLEDGMENTS

The authors gratefully acknowledge discussions with D. L. Smith of Los Alamos National Laboratory and Christian Mailhiot of Xerox Corporation. Discussions with Ogden Marsh and Mary Young of Hughes Research Laboratories have enhanced our understanding of possible infrared applications for this superlattice. Useful advice and assistance was provided by A. T. Hunter, J. P. Baukus, C. Haeussler, D. A. Collins, and L. R. Dawson. The support of the Defense Advanced Research Projects Agency under Grant Nos. N00014-89-J-3196 and N00014-89-C-0203 has made it possible for us to carry out this program. One of us (D. H. C.) was supported in part by Caltech's Program in Advanced Technologies, sponsored by Aerojet General, General Motors, and TRW.

[a] Present address: Chalmers University of Technology, Department of Physics, S-41296, Göteborg, Sweden.

[1] J. N. Schulman and T. C. McGill, Appl. Phys. Lett. **34**, 663 (1979).
[2] D. L. Smith, T. C. McGill, and J. N. Schulman, Appl. Phys. Lett. **43**, 160 (1983).
[3] G. C. Osbourn, J. Vac. Sci. Technol. B **2**, 176 (1984).
[4] S. R. Kurtz, G. C. Osbourn, R. M. Biefeld, L. R. Dawson, and H. J. Stein, Appl. Phys. Lett. **52**, 831 (1988).
[5] S. R. Kurtz, L. R. Dawson, R. M. Biefeld, I. J. Fritz, and T. E. Zipperian, IEEE Electron Device Lett. **10**, 150 (1989).
[6] D. L. Smith and C. Mailhiot, J. Appl. Phys. **62**, 2545 (1987).
[7] C. Mailhiot and D. L. Smith, J. Vac. Sci. Technol. A **7**, 445 (1989).
[8] G. A. Sai-Halasz, L. L. Chang, J.-M. Welter, C.-A. Chang, and L. Esaki, Solid State Commun. **27**, 935 (1978).
[9] P. Voisin, G. Bastard, C. E. T. Goncalves da Silva, M. Voos, L. L. Chang, and L. Esaki, Solid State Commun. **39**, 79 (1981).
[10] D. K. Arch, G. Wicks, T. Tonaue, J.-L. Staudenmann, J. Appl. Phys. **58**, 3933 (1985).
[11] W. K. Chu, F. W. Saris, C.-A. Chang, R. Ludeke, and L. Esaki, Phys. Rev. B **26**, 1999 (1982).
[12] L. L. Chang and L. Esaki, Surf. Sci. **98**, 70 (1980).
[13] B. C. DeCooman, C. B. Carter, G. W. Wicks, T. Tanoue, and L. F. Eastman, Thin Solid Films **170**, 49 (1989).
[14] J. Bleuse, P. Voisin, M. Voos, H. Munekata, L. L. Chang, and L. Esaki, Appl. Phys. Lett. **52**, 462 (1988).
[15] S. Kalem, J. I. Chyi, H. Morkoç, R. Bean, and K. Zanio, Appl. Phys. Lett. **53**, 1648 (1988).
[16] J. R. Söderström, D. H. Chow, and T. C. McGill, Mat. Res. Soc. Symp. Proc. **145**, 409 (1989).
[17] M. Y. Yen, B. F. Levine, C. G. Bethea, K. K. Choi, and A. Y. Cho, Appl. Phys. Lett. **50**, 927 (1987).
[18] L. R. Dawson (private communication).
[19] B. M. Clemens and J. G. Gay, Phys. Rev. B **35**, 9337 (1987).